A new yield function for geomaterials.

Davide Bigoni[†]**, Andrea Piccolroaz**[†]

[†] *Dipartimento di Ingegneria Meccanica e Strutturale*
Università degli Studi di Trento, Italy

ABSTRACT. *A new yield function is proposed for modelling the inelastic behaviour of geomaterials and, more in general, quasibrittle and frictional materials, including soils, rocks, concrete, metallic and composite powders, metallic foams, porous metals, and polymers. The yield function represents a single, convex and smooth surface in stress space approaching as limit situations "classical" criteria and the extreme limits of convexity of deviatoric section. The yield function is therefore a generalization of several criteria, including von Mises, Drucker-Prager, Tresca, modified Tresca, Coulomb-Mohr, modified Cam-clay, and —concerning the deviatoric section— Rankine and Ottosen.*

Constitutive modelling and analysis of boundary value problems in geotechnical engineering
A workshop in Napoli, 22-24 April 2003, Viggiani, C. (ed)

1. Introduction

Yielding or damage of quasibrittle and frictional materials (a collective denomination for soil, concrete, rock, granular media, coal, cast iron, ice, porous metals, metallic foams, as well as certain types of ceramic) is complicated by many effects, including dependence on the first and third stress invariants (the so-called 'pressure-sensitivity' and 'Lode-dependence' of yielding), and represents the subject of an intense research effort. Restricting the attention to the formulation of yield criteria, research moved in two directions: one was to develop such criteria on the basis of micromechanics considerations, while another was to find direct interpolations to experimental data. Examples of yield functions generated within the former approach are numerous and, as a paradigmatic case, we may mention the celebrated Gurson criterion (Gurson, 1977). The latter approach was also broadly followed, providing some very successful yield condition, such as for instance the Ottosen criterion for concrete (Ottosen, 1977). Although very fundamental in essence, the micromechanics approach has however limits, particularly when employed for geomaterials. For instance, it is usually based on variational formulations possible —for inelastic materials— only for solids obeying the postulate of maximum dissipation at a microscale, which is typically violated for frictional materials such as for instance soils.

A purely phenomenological point of view is assumed in the present article, where a new yield function[1] is formulated, tailored to interpolate experimental results for quasibrittle and frictional materials, under the assumption of isotropy. The interest in this proposal lies in the features evidenced by the criterion. These are:

– closure both in tension and in compression;

– non-circular deviatoric section of the yield surface, which may approach both the upper and lower convexity limits for extreme values of material parameters;

– smoothness of the yield surface;

– extreme variation in shape of the yield surface and related capability of interpolating a broad class of experimental data for different materials;

– reduction to known-criteria in limit situations;

– convexity of the yield function (and thus of the yield surface);

– simple mathematical expression.

None of the above features is *essential*, in the sense that a plasticity theory can be developed without all of the above, but all are *desirable* for the development of certain models of interest, particularly in the field of geomaterials.

1. We do not need to distinguish here between yield, damage and failure. Within a phenomenological approach, all these situations are based on the concept of stress range, bounded by a given hypersurface defined in stress space.

The range of material parameters corresponding to convexity of the proposed yield function has been obtained by the autors in a related work (to appear), in which two general propositions have been developed, that can be useful for analyzing convexity of a broad class of yield functions. The propositions are shown to be constructive, in the sense that these may be employed to generate convex yield functions.

2. Notation

The analysis will be restricted to isotropic behaviour, therefore the Haigh-Westergaard representation of the yield locus is employed (Hill, 1950). This is well-known, so that we limit the presentation here to a few remarks that may be useful in the following. First, we recall that:

$\mathcal{A}1$. a single point in the Haigh-Westergaard space is representative of the infinite (to the power three) stress tensors having the same principal values;

$\mathcal{A}2$. due to the arbitrary in the numeration of the eigenvalues of a tensor, six different points correspond in the Haigh-Westergaard representation to a given stress tensor. As a result, the yield surface results symmetric about the projections of the principal axes on the deviatoric plane (Fig. 1);

$\mathcal{A}3$. the Haigh-Westergaard representation preserves the scalar product only between coaxial tensors;

$\mathcal{A}4$. a convex yield surface —for a material with a fixed yield strength under triaxial compression— must be internal to the two limit situations shown in Fig. 1 (Haythornthwaite, 1985). Note that the inner bound will be referred as 'the Rankine limit'.

Due to isotropy, the analysis of yielding can be pursued fixing once and for all a reference system and restricting to all stress tensors diagonal in this system. We will refer to this setting as to the Haigh-Westergaard representation. When tensors (for instance, the yield function gradient) coaxial to the reference system are represented, the scalar product is preserved, property $\mathcal{A}3$. In the Haigh-Westergaard representation, the hydrostatic and deviatoric stress components are defined by the invariants

$$p = -\frac{\mathsf{tr}\,\boldsymbol{\sigma}}{3}, \quad q = \sqrt{3J_2}, \tag{1}$$

where

$$J_2 = \frac{1}{2}\mathbf{S}\cdot\mathbf{S}, \quad \mathbf{S} = \boldsymbol{\sigma} - \frac{\mathsf{tr}\,\boldsymbol{\sigma}}{3}\mathbf{I}, \tag{2}$$

in which $\mathbf{S}$ is the deviatoric stress, $\mathbf{I}$ is the identity tensor, a dot denotes scalar product and tr denotes the trace operator, so that $\mathbf{A}\cdot\mathbf{B} = \mathsf{tr}\,\mathbf{A}\mathbf{B}^T$, for every second-order

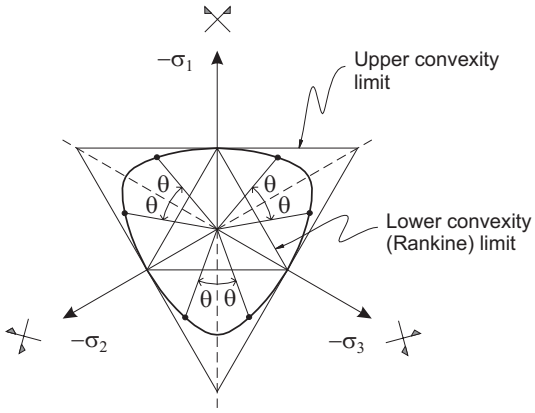

Figure 1. Deviatoric section: definition of angle θ, symmetries, lower and upper convexity bounds.

tensors $\mathbf{A}$ and $\mathbf{B}$. The position of the stress point in the deviatoric plane is singled out by the Lode (1926) angle θ defined as

$$\theta = \frac{1}{3}\cos^{-1}\left(\frac{3\sqrt{3}}{2}\frac{J_3}{{J_2}^{3/2}}\right), \quad J_3 = \frac{1}{3}\,\mathrm{tr}\,\mathbf{S}^3, \tag{3}$$

so that $\theta \in [0, \pi/3]$. As a consequence of property $(\mathcal{A}2)$ of the Haigh-Westergaard representation, a single value of θ corresponds to six different points in the deviatoric plane (Fig. 1). The following gradients of the invariants, that will be useful later,

$$\begin{aligned} &\frac{\partial p}{\partial \boldsymbol{\sigma}} = -\frac{1}{3}\mathbf{I}, \;\; \frac{\partial J_2}{\partial \boldsymbol{\sigma}} = \mathbf{S}, \;\; \frac{\partial J_3}{\partial \boldsymbol{\sigma}} = \mathbf{S}^2 - \frac{\mathrm{tr}\,\mathbf{S}^2}{3}\mathbf{I}, \\ &\frac{\partial \theta}{\partial \boldsymbol{\sigma}} = -\frac{9}{2\,q^3\,\sin 3\theta}\left(\mathbf{S}^2 - \frac{\mathrm{tr}\,\mathbf{S}^2}{3}\mathbf{I} - q\frac{\cos 3\theta}{3}\mathbf{S}\right), \end{aligned} \tag{4}$$

can be obtained from well-known formulae (e.g. Truesdell and Noll, 1965, Sect. 9) using the identity

$$\frac{\partial \mathbf{S}}{\partial \boldsymbol{\sigma}} = \mathbf{I}\,\underline{\overline{\otimes}}\,\mathbf{I} - \frac{1}{3}\mathbf{I}\otimes\mathbf{I}, \tag{5}$$

where the symbol $\otimes$ denotes the usual dyadic product and $\mathbf{I}\,\underline{\overline{\otimes}}\,\mathbf{I}$ is the symmetrizing fourth-order tensor, defined for every tensor $\mathbf{A}$ as $\mathbf{I}\,\underline{\overline{\otimes}}\,\mathbf{I}[\mathbf{A}] = (\mathbf{A} + \mathbf{A}^T)/2$. Note that $\partial\theta/\partial\boldsymbol{\sigma}$ is orthogonal to $\mathbf{I}$ and to the deviatoric stress $\mathbf{S}$.

3. A new yield function

We propose the seven-parameters yield function $F : \mathsf{Sym} \to \mathbb{R} \cup \{+\infty\}$ defined as:

$$F(\boldsymbol{\sigma}) = f(p) + \frac{q}{g(\theta)}, \tag{6}$$

where the dependence on the stress $\boldsymbol{\sigma}$ is included in the invariants p, q and θ, eqns (1) and (3), through the 'meridian' function

$$f(p) = \begin{cases} -Mp_c\sqrt{(\Phi - \Phi^m)\left[2(1-\alpha)\Phi + \alpha\right]} & \text{if } \Phi \in [0,1], \\ +\infty & \text{if } \Phi \notin [0,1], \end{cases} \tag{7}$$

where

$$\Phi = \frac{p + c}{p_c + c}, \tag{8}$$

describing the pressure-sensitivity and the 'deviatoric' function

$$g(\theta) = \frac{1}{\cos\left[\beta\frac{\pi}{6} - \frac{1}{3}\cos^{-1}\left(\gamma\cos 3\theta\right)\right]}, \tag{9}$$

describing the Lode-dependence of yielding. The seven, non-negative material parameters:

$$\underbrace{M > 0,\ p_c > 0,\ c \geq 0,\ 0 < \alpha < 2,\ m > 1}_{\text{defining } f(p)},\quad \underbrace{0 \leq \beta \leq 2,\ 0 \leq \gamma < 1}_{\text{defining } g(\theta)}, \tag{10}$$

define the shape of the associated (single, smooth) yield surface. In particular, M controls the pressure-sensitivity, p_c and c are the yield strengths under isotropic compression and tension, respectively. Parameters α and m define the distortion of the meridian section, whereas β and γ model the shape of the deviatoric section. Note that the deviatoric function describes a piecewise linear deviatoric surface in the limit $\gamma \longrightarrow 1$. Finally, it is important to remark that within the interval of $\beta \in [0, 2]$ the yield function is convex independently of the values assumed by parameter γ. Convexity requirements, that will be proved later, impose a broader variation of β than $(10)_6$, but the interval where β may range becomes a function of γ. In particular, the yield function is convex when

$$2 - \mathcal{B}(\gamma) \leq \beta \leq \mathcal{B}(\gamma), \tag{11}$$

where function $\mathcal{B}(\gamma)$ takes values within the interval $]2, 4]$, when γ ranges in $[0, 1[$ and is defined as

$$\mathcal{B}(\gamma) = 3 - \frac{6}{\pi}\tan^{-1}\left.\frac{1 - 2\cos z - 2\cos^2 z}{2\sin z(1 - \cos z)}\right|_{z=2/3(\pi - \cos^{-1}\gamma)}. \tag{12}$$

The yield function (6) corresponds to the following yield surface:

$$q = -f(p)g(\theta), \quad p \in [-c, p_c], \;\; \theta \in [0, \pi/3], \tag{13}$$

which makes explicit the fact that $f(p)$ and $g(\theta)$ define the shape of the meridian and deviatoric sections, respectively.

The yield surface (13) is sketched in Figs. 2-3 for different values of the seven above-defined material parameters (non-dimensionalization is introduced through division by p_c in Fig. 2). In particular, meridian sections are reported in Figs. 2, whereas Fig. 3 pertains to deviatoric sections.

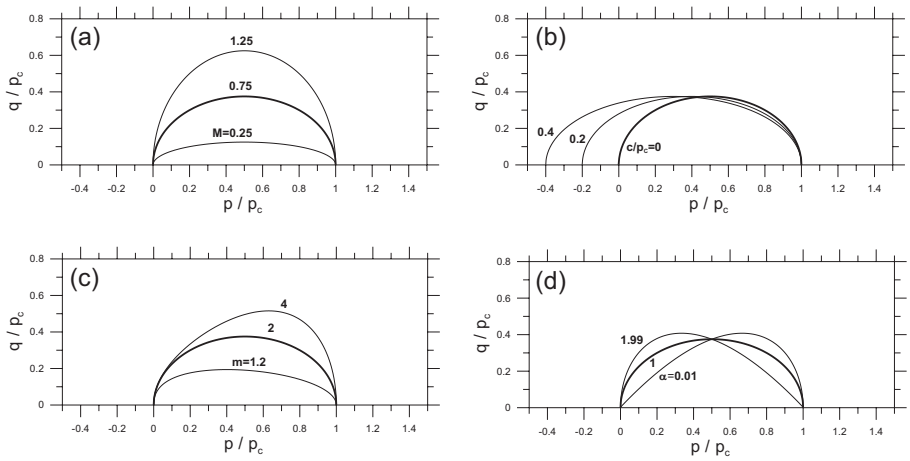

Figure 2. Meridian section: effects related to the variation of parameters M (a), c/p_c (b), m (c), and α (d).

As a reference, the case corresponding to the modified Cam-clay introduced by Roscoe and Burland (1968) and Schofield and Wroth (1968) and corresponding to $\beta = 1$, $\gamma = 0$, $\alpha = 1$, $m = 2$, and $c = 0$ is reported in Fig. 2 as a solid line, for $M = 0.75$. The distortion of meridian section reported in Fig. 2(a) —where $M = 0.25, 0.75, 1.25$— can also be obtained within the framework of the modified Cam-clay, whereas the effect of an increase in cohesion reported in Fig. 2(b) —where $c/p_c = 0, 0.2, 0.4$— may be employed to model the gain in cohesion consequent to plastic strain, during compaction of powders.

The shape distortion induced by the variation of parameters m and α, Fig. 2(c) —where $m = 1.2, 2, 4$— and 2(d) —where $\alpha = 0.01, 1.00, 1.99$— is crucial to fit experimental results relative to frictional materials.

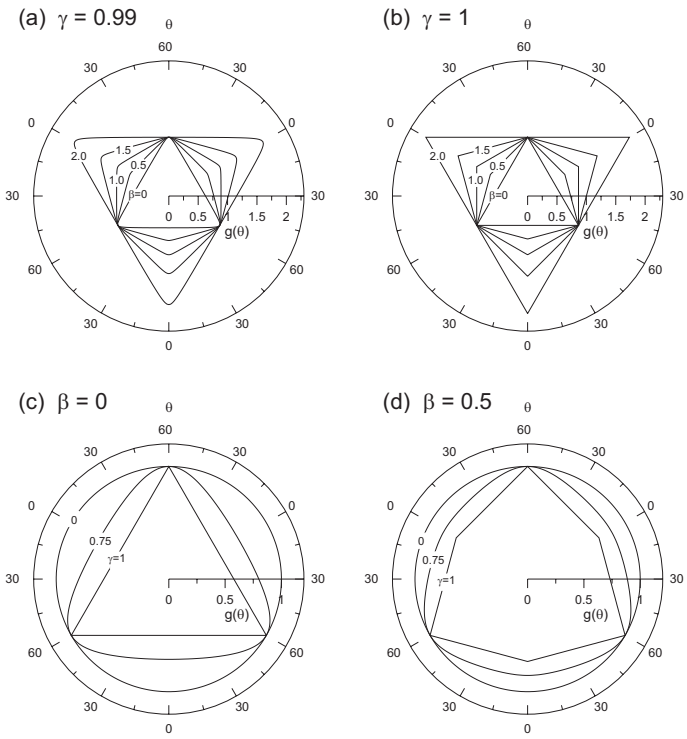

Figure 3. Deviatoric section: effects related to the variation of β and γ. Variation of $\beta = 0, 0.5, 1, 1.5, 2$ at fixed $\gamma = 0.99$ (a) and $\gamma = 1$ (b). Variation of $\gamma = 1, 0.75, 0$ at fixed $\beta = 0$ (c) and $\beta = 0.5$ (d).

The possibility of extreme shape distortion of the deviatoric section, which may range between the upper and lower convexity limits, and approach Tresca, von Mises and Coulomb-Mohr, is sketched in Fig. 3. It should be noted that to simplify reading of the figure, function $g(\theta)$ has been normalized through division by $g(\pi/3)$, so that all deviatoric sections coincide at the point $\theta = \pi/3$. Parameter γ is kept fixed in Figs. 3 (a) and (b) and equal to 0.99 and 1, respectively, whereas parameter β is fixed in Figs. 3 (c) and (d) and equal to 0 and 1/2. Therefore, figures (a) and (b) demonstrate the effect of the variation in β (= 0, 0.5, 1, 1.5, 2) which makes possible a distortion of the yield surface from the upper to lower convexity limits going through Tresca and Coulomb-Mohr shapes. The role played by γ (= 1, 0.75, 0) is investigated in figures (c) and (d), from which it becomes evident that γ has a smoothing effect on the corners, emerging in the limit $\gamma = 1$. The von Mises (circular) deviatoric section emerges when $\gamma = 0$.

The yield surface in the biaxial plane σ_1 versus σ_2, with $\sigma_3 = 0$ is sketched in Fig. 4, where axes are normalized through division by the uniaxial tensile strength f_t.

In particular, the figure pertains to $M = 0.75$, $p_c = 50c$, $m = 2$, and $\alpha = 1$, whereas $\gamma = 0.99$ is fixed and β is equal to {0, 0.5, 1, 1.5, 2} in Fig. 4(a) and, vice-versa, $\beta = 0$ is fixed and γ is equal to {0, 0.75, 0.99} in Fig. 4(b).

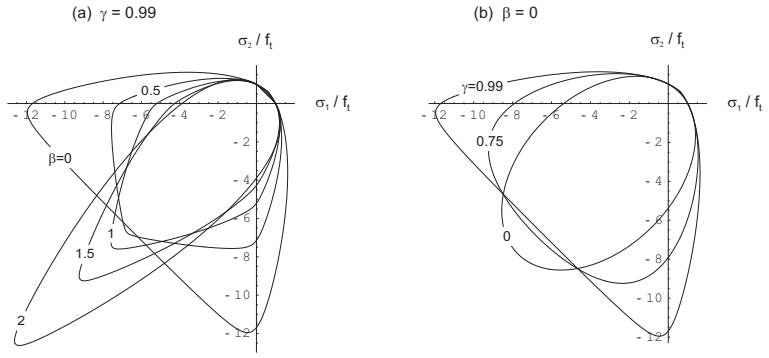

Figure 4. Yield surface in the biaxial plane σ_1/f_t vs. σ_2/f_t, with $\sigma_3 = 0$. Variation of $\beta = 0, 0.5, 1, 1.5, 2$ at fixed $\gamma = 0.99$ (a) and variation of $\gamma = 0, 0.75, 0.99$ at fixed $\beta = 0$ (b).

3.1. *Reduction of yield criterion to known cases*

The yield function (6)-(9) reduces to almost all[2] 'classical' criteria of yielding. These can be obtained as limit cases in the way illustrated in Tab. 1 where the modified Tresca criterion was introduced by Drucker (1953), whereas the Haigh-Westergaard representation of the Coulomb-Mohr criterion was proposed by Shield (1955). In Tab. 1 parameter r denotes the ratio between the uniaxial strengths in compression (taken positive) and tension, indicated by f_c and f_t, respectively. We note that for real materials $r \geq 1$ and that we did not explicitly consider the special cases of no-tension $f_t = 0$ or granular $f_t = f_c = 0$ materials [which anyway can be easily incorporated as limits of (6)-(9)].

We note that the expression of the Tresca criterion which follows from (6)-(9) in the limits specified in Tab. 1, was provided also by Bardet (1990) and answers — in a positive way— the question (raised by Salençon, 1974) if a proper form of the criterion in terms of stress invariants exist.

2. A remarkable exception is the isotropic Hill (1950 b) criterion, corresponding to a Tresca criterion rotated of $\pi/6$ in the deviatoric plane.

Table 1. Yield criteria obtained as special cases of (6)-(9), $r = f_c/f_t$ and f_c and f_t are the uniaxial strengths in compression and tension, respectively.

Criterion	Meridian function $f(p)$	Deviatoric function $g(\theta)$
von Mises	$\alpha = 1, \quad m = 2,$ $M = \dfrac{2f_t}{p_c}, \quad c = p_c \longrightarrow \infty$	$\beta = 1, \gamma = 0$
Drucker-Prager	$\alpha = 0, \quad M = \dfrac{3(r-1)}{\sqrt{2}(r+1)},$ $c = \dfrac{2f_c}{3(r-1)}, \quad p_c = f_c\, m \longrightarrow \infty$	as for von Mises
Tresca	as for von Mises, except that $M = \dfrac{\sqrt{3}f_t}{p_c}$	$\beta = 1, \gamma \longrightarrow 1$
mod. Tresca	as for Drucker-Prager, except that $M = \dfrac{3\sqrt{3}(r-1)}{2\sqrt{2}(r+1)}$	as for Tresca
Coulomb-Mohr	as for Drucker-Prager, except that $M = \dfrac{3\left[r\cos\left(\beta\frac{\pi}{6} - \frac{\pi}{3}\right) - \cos\beta\frac{\pi}{6}\right]}{\sqrt{2}(r+1)}$ $c = \dfrac{f_c\left[\cos\left(\beta\frac{\pi}{6} - \frac{\pi}{3}\right) + \cos\beta\frac{\pi}{6}\right]}{3r\cos\left(\beta\frac{\pi}{6} - \frac{\pi}{3}\right) - 3\cos\beta\frac{\pi}{6}}$	$\beta = \dfrac{6}{\pi}\tan^{-1}\dfrac{\sqrt{3}}{2r+1},$ $\gamma \longrightarrow 1$
mod. Cam-clay	$m = 2,\ \alpha = 1,\ c = 0$	as for von Mises

The Mohr-Coulomb limit merits a special mention. In fact, if the following values of the parameters are selected

$$\begin{aligned} &\alpha = 0, \quad c = \frac{f_c\left[\cos\left(\beta\frac{\pi}{6} - \frac{\pi}{3}\right) + \cos\beta\frac{\pi}{6}\right]}{3r\cos\left(\beta\frac{\pi}{6} - \frac{\pi}{3}\right) - 3\cos\beta\frac{\pi}{6}}, \\ &M = \frac{3\left[r\cos\left(\beta\frac{\pi}{6} - \frac{\pi}{3}\right) - \cos\beta\frac{\pi}{6}\right]}{\sqrt{2}(r+1)}, \end{aligned} \tag{14}$$

and then the limits

$$\gamma \longrightarrow 1, \quad p_c = f_c\, m \longrightarrow \infty, \tag{15}$$

are performed, a three-parameters generalization of Coulomb-Mohr criterion is obtained, which reduces to the latter criterion in the special case when β is selected in the form specified in Tab. 1 (yielding an expression noted also by Chen and Saleeb, 1982). The cases reported in Tab. 1 refer to situations in which the criterion (6)-(9) reduces to known yield criteria both in terms of function $f(p)$ and of function $g(\theta)$. It is however important to mention that the Lode's dependence function $g(\theta)$ reduces also to well-known cases, but in which the pressure-sensitivity cannot be described by the meridian function (7). These are reported in Tab. 2. It is important to mention that the form of our function $g(\theta)$, eqn. (9), was indeed constructed as a generalization of the deviatoric function introduced by Ottosen (1977).

Table 2. Deviatoric yield functions obtained as special cases of (9)

Criterion	Deviatoric function $g(\theta)$
Lower convexity (Rankine)	$\beta = 0,\ \gamma \longrightarrow 1$
Upper convexity	$\beta = 2,\ \gamma \longrightarrow 1$
Ottosen	$\beta = 0,\ 0 \leq \gamma < 1$

3.2. *A comparison with experiments*

A brief comparison with experimental results referred to several materials is reported below. We limit the presentation to a few representative examples demonstrating the extreme flexibility of the proposed model to fit experimental results. In particular, we concentrate on the meridian section, whereas only few examples are provided for the deviatoric section, which has a shape so deformable and ranging between well-known forms that fitting experiments is a-priori expected. Results on the biaxial plane $\sigma_1 - \sigma_2$ are also included.

Typical of soils are the experimental results reported in Fig. 5, on Aio sand and Weald clay, taken, respectively, from Yasufuku et al. (1991, their Fig. 10a) and Parry (reported by Wood, 1990, their Fig. 7.22, so that p_e is the equivalent consolidation pressure in Fig. 5(b)). Note that the upper plane of the graphs refers to triaxial compression ($\theta = \pi/3$), whereas triaxial extension is reported in the lower part of the graphs ($\theta = 0$). It may be concluded from the figure that experimental results can be easily fitted by our function $f(p)$, still maintaining a smooth intersection of the yield surface with $p-$axis.

In addition to soils, the proposed function (6)-(9) can model yielding of porous ductile or cellular materials, metallic and composite powders, concrete and rocks. To further develop this point, a comparison with experimental results given by Sridhar

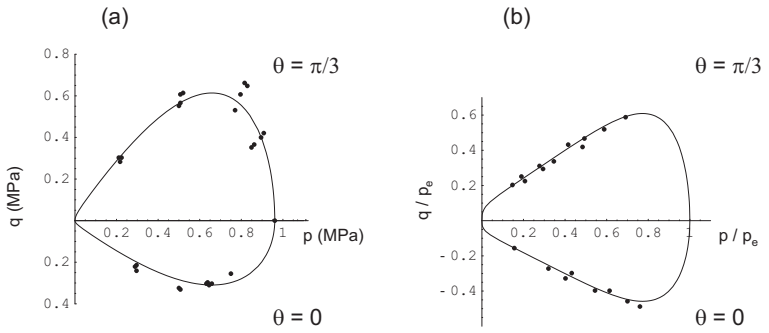

Figure 5. Comparison with experimental results relative to sand (Yasufuku et al. 1991) (a) and clay (Parry, reported by Wood, 1990) (b).

and Fleck (2000) —their Figs. 5(b) and 9(c)— relative to ductile powders is reported in Fig. 6. In particular, Fig. 6(a) is relative to an aluminum powder (Al D_0=0.67, D=0.81 in Sridhar and Fleck, their Fig. 5b), Fig. 6(b) to an aluminum powder reinforced by 40 vol.%SiC (Al-40%Sic D_0=0.66, D=0.82 in Sridhar and Fleck, their Fig. 5b), Fig. 6(c) to a lead powder (0% steel in Sridhar and Fleck, their Fig. 9c), and Fig. 6(d) to a lead shot-steel composite powder (20% steel in Sridhar and Fleck, their Fig. 9c). Beside the fairly good agreement between experiments and proposed yield function, we note that the aluminium powder has a behaviour —different from soils and lead-based powders— resulting in a meridian section of the yield surface similar to the early version of the Cam-clay model (Roscoe and Schofield, 1963).

Regarding concrete, among the many experimental results currently available, we have referred to Sfer et al. (2002, their Fig. 6) and to the Newman and Newman (1971) empirical relationship

$$\frac{\sigma_1}{f_c} = 1 + 3.7 \left(\frac{\sigma_3}{f_c} \right)^{0.86}, \tag{16}$$

where σ_1 and σ_3 are the maximum and minimum principal stresses at failure and f_c is the value of the ultimate uniaxial compressive strength. Small circles in Fig. 7 represents results obtained using relationship (16) in figure (a) and experimental results by Sfer et al. (2002) in figure (b); the approximation provided by the criterion (7)-(8) is also reported as a continuous line.

As far as rocks are concerned, we limit to a few examples. However, we believe that due to the fact that our criterion approaches Coulomb-Mohr, it should be particularly suited for these materials. In particular, data taken from Hoek and Brown (1980, their pages 143 and 144) are reported in Fig. 8 as small circles for two rocks, chert (Fig. 8a) and dolomite (Fig. 8b).

A few data on polymers are reported in Fig. 9 —together with the fitting provided by our model— concerning polymethil methacrylate (Fig. 9a) and an epoxy binder

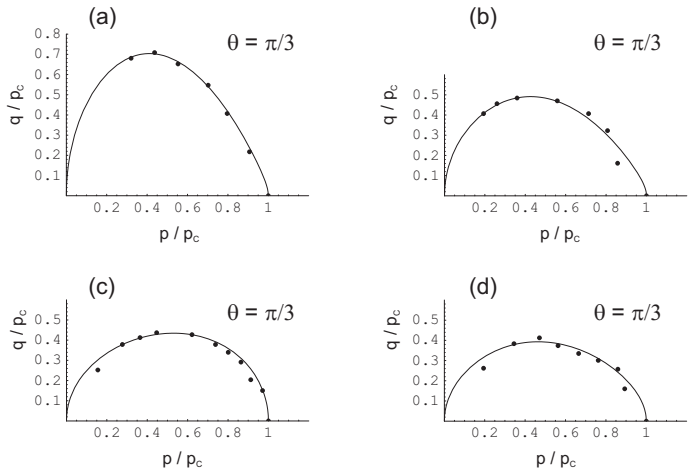

Figure 6. Comparison with experimental results relative to aluminium powder (a) aluminum composite powder (b), lead powder (c) and lead shot-steel composite powder(d), data taken from Sridhar and Fleck (2000).

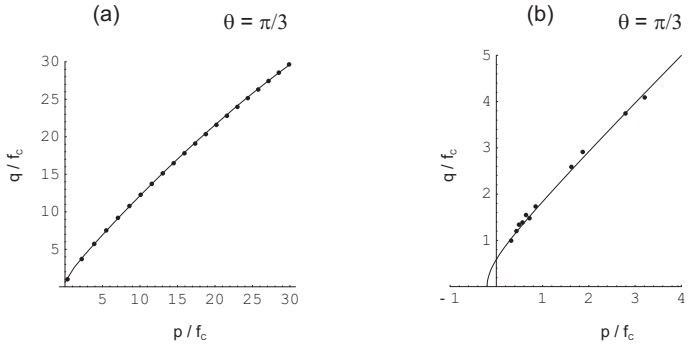

Figure 7. Comparison with the experimental relation (16) proposed by Newman and Newman (1971) (a) and with results by Sfer et al. (2002) (b).

(Fig. 9b), taken from Ol'khovik (1983, their Fig. 5), see also Altenbach and Tushtev (2001, their Figs. 2 and 3).

Finally, our model describes —with a different yield function— the same yield surface proposed by Deshpande and Fleck (2000) to describe the behaviour of metallic foams. In particular, the correspondence between parameters of our model (6)-(9) and

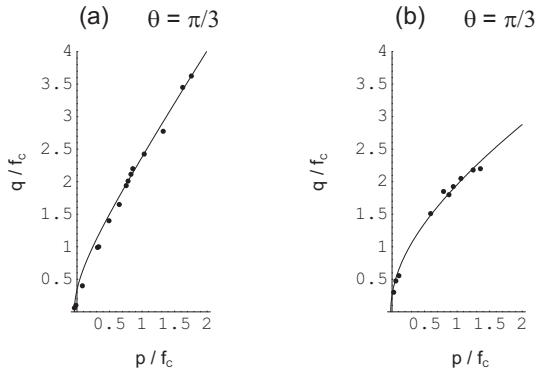

Figure 8. Comparison with experiments for rocks. Chert (a) and dolomite (b), data taken from Hoek and Brown (1980).

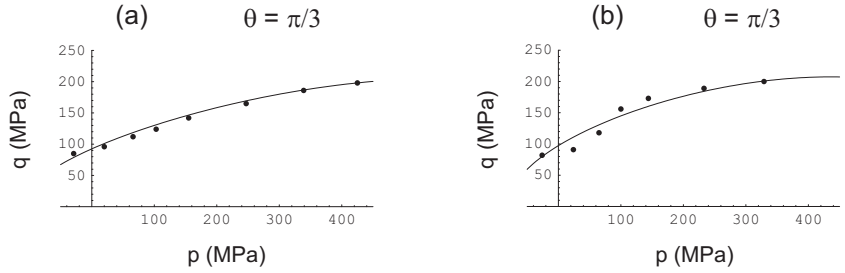

Figure 9. Comparison with experimental results for polymers. Methacrylate (a) and an epoxy binder (b), data taken from Ol'khovik (1983).

of the yield surface proposed by Deshpande and Fleck [2000, their eqns. (2)-(3)] is obtained setting

$$\beta = 1, \quad \gamma = 0, \quad m = 2, \quad \alpha = 1,$$

and assuming the correlations given in Tab. 3.

The proposed function (6)-(9) is also expected to model correctly yielding of porous ductile metals. As a demonstration of this, we present in Fig. 10 a comparison with the Gurson (1977) model. The Gurson yield function has a circular deviatoric section so that $\beta = 1$ and $\gamma = 0$ in our model, in addition, we select

$$\begin{aligned} &\alpha = 1, \quad m = 2, \quad p_c = c = \sigma_M \frac{2}{3q_2} \cosh^{-1} \frac{1 + q_3 f^2}{2 f q_1}, \\ &M = \sigma_M \frac{2}{p_c} \sqrt{1 + q_3 f^2 - 2 f q_1}, \end{aligned} \tag{17}$$

Table 3. Correspondence between parameters of (6)-(9) and Deshpande and Fleck (2002) yield functions —the latter shortened as 'DF model'— to describe the behaviour of metallic foams.

	Model (6)-(9)			DF model	
	M	c	p_c	Y	α
DF model Y, α	2α	$\frac{Y}{\alpha}\sqrt{1+\left(\frac{\alpha}{3}\right)^2}$	$\frac{Y}{\alpha}\sqrt{1+\left(\frac{\alpha}{3}\right)^2}$	—	—
Model (6)-(9) M, p_c, c	—	—	—	$\frac{cM}{2\sqrt{1+\left(\frac{M}{6}\right)^2}}$	$\frac{M}{2}$

where f is the void volume fraction (taking the values {0.01, 0.1, 0.3, 0.6 } in Fig. 10), σ_M is the equivalent flow stress in the matrix material and $q_1 = 1.5$, $q_2 = 1$ and $q_3 = q_1^2$ are the parameters introduced by Tvergaard (1981, 1982). A good agreement between the two models can be appreciated from Fig. 10, increasing when the void volume fraction f increases.

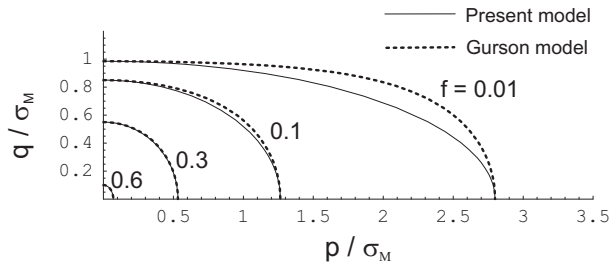

Figure 10. Comparison with the Gurson model at different values of void volume fraction f.

As far as the deviatoric section is regarded, we limit to two examples —reported in Fig. 11— concerning sandstone and dense sand, where the experimental data have been taken from Lade (1997, their Figs. 2 and 9a).

Experimental data referred to the biaxial plane $\sigma_3 = 0$ for grey cast iron and concrete (taken respectively from Coffin and Schenectady, 1950, their Fig. 5 and Tasuji et al. 1978, their Figs. 1 and 2) are reported in Fig. 12.

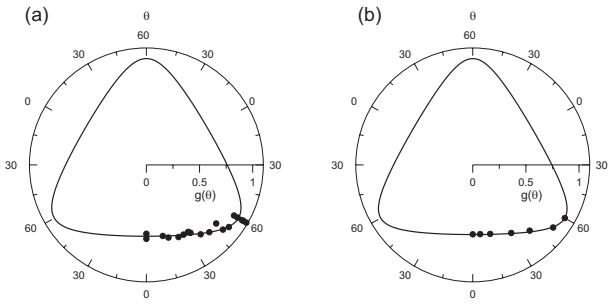

Figure 11. Comparison with experimental results relative to deviatoric section for sandstone (a) and dense sand (b) data taken from (Lade, 1997).

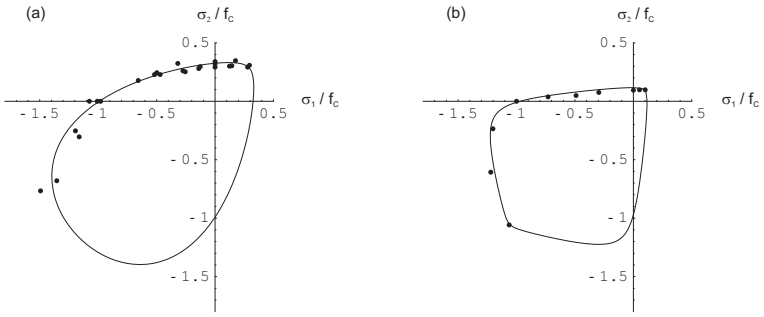

Figure 12. Comparison with experimental results on biaxial plane for cast iron (data taken from Coffin and Schenectady, 1950)(a) and concrete (data taken from Tasuji et al. 1978)(b).

4. Conclusions

In the modelling of the inelastic behaviour of several materials, the knowledge of a smooth yield surface approaching know-criteria and possessing an extreme shape variation to fit experimental results may be very useful. In the present paper, such a yield function has been proposed, which is shown to be capable of an accurate description of the behaviour of a broad class of materials including soils, concrete, rocks, powders, metallic foams, porous materials, and polymers.

References

Altenbach, H., Tushtev, K., 2001, A new static failure criterion for isotropic polymers, *Mech. Compos. Mater.*, **37**, 475-482.

Bardet, J.P., 1990, Lode dependences for isotropic pressure-sensitive elastoplastic materials, *J. Appl. Mech.*, **57**, 498-506.

Chen, W.F., Saleeb, A.F., 1982, Constitutive equations for engineering materials: elasticity and modelling, Wiley & Sons, New York.

Coffin, L.F., Schenectady, N.Y., 1950, The flow and fracture of a brittle material, *J. Appl. Mech.*, **17**, 233-248.

Deshpande, V.S., Fleck, N.A., 2000, Isotropic constitutive models for metallic foams, *J. Mech. Phys. Solids*, **48**, 1253-1283.

Drucker, D.C., 1953, Limit analysis of two and three dimensional soil mechanics problems, *J. Mech. Phys. Solids*, **1**, 217-226.

Gurson, A.L., 1977, Continuum theory of ductile rupture by void nucleation and growth: part I, yield criteria and flow rules for porous ductile media, *Int. J. Engng. Mat. Tech.*, **99**, 2-15.

Haythornthwaite, R.M., 1985, A family of smooth yield surfaces, *Mechanics Research Communications*, **12**, 87-91.

Hill, R., 1950 a, The mathematical theory of plasticity, Clarendon Press, Oxford.

Hill, R., 1950 b, Inhomogeneous deformation of a plastic lamina in a compression test, *Phil. Mag.*, **41**, 733-744.

Hoek, E., Brown, E.T., 1980, Underground excavations in rock, The Institution of Mining and Metallurgy, London.

Lade P.V., 1997, Modelling the strengths of engineering materials in three dimensions, *Mech. Cohes. Fricct. Mat.*, **2**, 339-356.

Lode, W., 1926, Versuche über den Einfluß der mittleren Hauptspannung auf das Fließen der Metalle Eisen Kupfer und Nickel, *Z. Physik.*, **36**, 913-939.

Newman, K., Newman, J.B., 1971, Failure theories and design criteria for plain concrete, in: Structure, Solid Mechanics and Engineering Design, *Proc. 1969 Southampton Civil Engineering Conf., Te'eni, M. Ed., Wiley Interscience, New York, pp. 963-995*.

Ol'khovik, O., 1983, Apparatus for testing of strength of polymers in a three-dimensional stressed state, *Mech. Compos. Mater.*, **19**, 270-275.

Ottosen, N.S., 1977, A failure criterion for concrete, *J. Eng. Mech. Div.-ASCE*, **103**, 527-535.

Roscoe, K.H., Burland, J.B., 1968, On the generalized stress-strain behaviour of 'wet' clay, Engineering Plasticity, Heyman, J. and Leckie, F.A., Eds., Cambridge University Press, Cambridge.

Roscoe, K.H., Schofield, A.N., 1963, Mechanical behaviour of an idealised 'wet' clay, *Proc. European Conf. on Soil Mechanics and Foundation Engineering, Wiesbaden (Essen: Deutsche Gesellshaft für Erd- und Grundbau e. V.), vol. 1, pp. 47-54*.

Salençon, J., 1974, Applications of the theory of plasticity in soil mechanics, Wiley & Sons, Chichester.

Schofield, A.N., Wroth, C.P., 1968, Critical state soil mechanics, McGraw-Hill Book Company, London.

Sfer, D., Carol, I., Gettu, R., Etse, G., 2002, Study of the behaviour of concrete under triaxial compression, *ASCE J. Engng. Mech.*, **128**, 156-163.

Shield, R.T., 1955, On Coulomb's law of failure in soils, *J. Mech. Phys. Solids*, **4**, 10-16.

Sridhar, I., Fleck, N.A., 2000, Yield behaviour of cold compacted composite powders, *Acta mater.*, **48**, 3341-3352.

Tasuji, M.E., Slate, F.O., Nilson, A.H., 1978, Stress-strain response and fracture of concrete in biaxial loading, *ACI J.*, **75**, 306-312.

Truesdell, C. and Noll, W., 1965, The non-linear field theories of mechanics, in Flügge, S., ed., Encyclopedia of Physics:III/3, Springer-Verlag, Berlin.

Tvergaard, V., 1981, Influence of voids on shear band instabilities under plane strain conditions, *Int. J. Fracture*, **17**, 389-407.

Tvergaard, V., 1982, On localization in ductile materials containing spherical voids, *Int. J. Fracture*, **18**, 237-252.

Wood, D.M., 1990, Soil behaviour and critical state soil mechanics, Cambridge University Press, Cambridge.

Yasufuku, N., Murata, H., Hyodo, M., 1991, Yield characteristics of anisotropically consolidated sand under low and high stress, *Soils and Foundations*, **31**, 95-109.